SENSITIVITY OF DIRECT GLOBAL WARMING POTENTIALS TO KEY UNCERTAINTIES *

D. J. WUEBBLES **, A. K. JAIN **, K. O. PATTEN ** and K. E. GRANT
Lawrence Livermore National Laboratory, Livermore, California, 94550, U.S.A.

Abstract. The concept of global warming potential was developed as a relative measure of the potential effects on climate of a greenhouse gas as compared to CO_2. In this paper a series of sensitivity studies examines several uncertainties in determination of Global Warming Potentials (GWPs). For example, the original evaluation of GWPs for the Intergovernmental Panel on Climate Change (IPCC, 1990) did not attempt to account for the possible sinks of carbon dioxide (CO_2) that could balance the carbon cycle and produce atmospheric concentrations of CO_2 that match observations. In this study, a balanced carbon cycle model is applied in calculation of the radiative forcing from CO_2. Use of the balanced model produces up to 21% enhancement of the GWPs for most trace gases compared with the IPCC (1990) values for time horizons up to 100 years, but a decreasing enhancement with longer time horizons. Uncertainty limits of the fertilization feedback parameter contribute a 20% range in GWP values. Another systematic uncertainty in GWPs is the assumption of an equilibrium atmosphere (one in which the concentration of trace gases remains constant) versus a disequilibrium atmosphere (one in which the concentration of trace gases varies with time). The latter gives GWPs that are 19 to 32% greater than the former for a 100 year time horizons, depending upon the carbon dioxide emission scenario chosen. Five scenarios are employed: constant-concentration, constant-emission past 1990 and the three IPCC (1992) emission scenarios. For the analysis of uncertainties in atmospheric lifetime (τ) the GWP changes in direct proportion to τ for short-lived gases, but to a lesser extent for gases with τ greater than the time horizontal for the GWP calculation.

1. Introduction

The Global Warming Potential (GWP) concept (IPCC, 1990) was developed at the request of policy makers as a relative measure of the potential effects on climate from various greenhouse gas emissions, in much the same way as the Ozone Depletion Potential concept (Wuebbles, 1981) is used in policy analyses of the relative effects of CFCs and other compounds on stratospheric ozone destruction. In order to evaluate the climatic implications of emission control strategies, GWPs can be used to calculate the required emission reduction for each greenhouse gas. The GWP of a greenhouse gas as defined in IPCC (1990) is the time-integrated change over specified time horizon in radiative forcing of a gas relative to that of CO_2:

$$GWP_i = \frac{\int_0^n a_i c_i \mathrm{d}t}{\int_0^n a_{CO_2} c_{CO_2} \mathrm{d}t}\,, \tag{1}$$

** Now at: Department of Atmospheric Sciences, University of Illinois, Urbana, Illinois, 61801, U.S.A.

Climatic Change **29:** 265–297, 1995.

where a_i is the radiative forcing change due to an instantaneous emission of 1 kg of gas i, c_i is the concentration of gas i remaining at time t, and n is the number of years over which the calculation is performed. The corresponding values for CO_2 are in the denominator; GWPs are defined relative to CO_2 because of its primary importance in concerns about future climate change. The definition above assumes a linear relationship between the incremental concentration change and the resulting change in radiative forcing. This is appropriate for the small emission impulse intended in the IPCC definition of GWPs. A more general definition of GWPs, used in the calculations presented in this paper, would be:

$$GWP_i = \frac{\int_0^n \Delta F_{c_i}(t)\mathrm{d}t}{\int_0^n \Delta F_{\mathrm{CO}_2}(t)\mathrm{d}t}, \tag{2}$$

where $\Delta F_{c_i}(t)$ is the change in radiative forcing due to an instantaneous emission of a unit mass of specie c_i. In these definitions, radiative forcing is defined by the net radiative flux change induced at the tropopause. We have recognized for some time that there are a number of uncertainties and limitations associated with the Global Warming Potential concept as defined in the IPCC reports. Some of the major uncertainties are briefly outlined below and in more detail in Harvey (1993).

Because GWPs are defined relative to CO_2, GWPs are quite sensitive to uncertainties in the treatment of the carbon cycle and its effects on the amount of atmospheric CO_2. Accurate calculation of the current concentration of CO_2 is one condition needed to insure that the response of the atmosphere to CO_2 with time is modeled correctly. However, previously published GWP studies (IPCC, 1990, 1992; WMO, 1992) obtain GWPs based on CO_2 response functions from models that do not correctly calculate the current CO_2 carbon budget based on a reasonable emission history ('unbalanced' models). To estimate the GWP values and the past and future CO_2 concentrations, a balanced carbon cycle model is required.

GWPs are quite sensitive to the assumed background for CO_2. A constant concentration background, as assumed in the IPCC and WMO studies, is clearly unrealistic. This assumption implies that the pulse is considered to be emitted into the equilibrium system. The carbon cycle system, however, is currently in a disequilibrium state as a result of past emissions, and in the foreseeable future the concentrations of CO_2 will likely continue to increase. Atmospheric disequilibrium affects the integrated radiative forcing of CO_2 and hence GWPs, because the dependence of radiative forcing of CO_2 on its concentration.

GWPs depend upon the change in concentration of a trace gas with time arising from the impulse emission of the gas. Behavior of an impulse of most trace gases is dependent on the atmospheric lifetime of the gas; atmospheric lifetime reflects the removal rate for a given gas by chemical reactions and physical processes. However, the normal assumption of a constant atmospheric lifetime is not a sufficient description of the response of the atmosphere to an impulse of major greenhouse gases because the lifetime of gases vary with time.

In this paper, we examine several of the major uncertainties that affect the values of GWPs. Included are the uncertainties in GWPs that arise from the uncertainties in (i) modeling the current carbon budget (unbalanced versus balanced carbon cycle); (ii) the choice of the background atmosphere for CO_2 (disequilibrium versus equilibrium background atmosphere); and (iii) the atmospheric lifetimes of non-CO_2 greenhouse gases (constant versus varying lifetime).

2. Modeling of Global Warming Potentials

The GWP calculation for a particular gas requires radiative forcings both for the gas of interest and for CO_2, the reference gas. In this study, GWPs are evaluated using the radiative forcing expressions of IPCC (1990; see their Tables 2.2 and 2.4) over integration time period of 500 yr. Although there are possible uncertainties associated with these expressions, we will not address those uncertainties in this paper. The IPCC-derived GWPs assume that the background atmosphere is in equilibrium (that background concentrations are constant over the GWP integration period). In our calculations, the equilibrium GWP takes the background concentration for a trace gas as that present in the atmosphere just before the impulse. The concentrations of radiatively active trace gases in the real atmosphere are expected to vary with time. These concentration changes affect radiative forcing of CO_2 and non-CO_2 greenhouse gases. We thus also calculate GWPs for which the background concentration of a trace gas varies with time depending upon assumed future emission scenarios, or disequilibrium GWPs. The current study addresses only the effect of disequilibrium in CO_2, and other gases are treated as if they were at equilibrium at the concentrations given in the IPCC (1992) standard atmosphere with atmospheric lifetimes according to WMO (1992) and IPCC (1992). The atmospheric lifetimes based on WMO (1992) are reproduced in Table I along with the estimated uncertainty ranges.

For the calculations of the impulse response functions, the mass released is set at 1000 kg for all gases except CO_2. For CO_2 we have used a 1 Gt pulse. The radiative forcing of CO_2 is sufficiently linear with respect to mass released for amounts up to 1 Gt of carbon (1 GtC, equal to 3.7×10^{12} kg of CO_2) and reducing the mass released below 1000 kg causes computational errors. Integrated radiative forcings of CO_2 are scaled by dividing the radiative forcing values by 3.7×10^{-9}.

3. Balancing the Carbon Cycle Model

For appropriately balancing the carbon cycle model, we need to remove any inconsistencies between model output and observations. When a balanced model is run from pre-industrial time to the current date using the published evaluations for changes in emissions (from fossil fuel burning and from land use changes), it

TABLE I

Atmospheric lifetimes for greenhouse gases (in years) and estimated uncertainty range (based on WMO, 1992; IPCC, 1992)

Gas	Lifetime	Range
CH_4	10.5	8.4–12.6
N_2O	132.0	110.0–168.0
CFC-11	55.0	42.0–66.0
CFC-12	116.0	95.0–130.0
CFC-113	110.0	75.0–144.0
CFC-114	220.0	197.0–264.0
CFC-115	550.0	400.0–800.0
HCFC-22	15.8	12.0–19.6
HCFC-123	1.7	1.3–2.1
HCFC-124	7.1	5.3–8.5
HFC-125	40.5	31.6–49.8
HFC-134a	15.6	11.3–21.1
HCFC-141b	11.4	9.1–12.5
HCFC-142b	22.6	17.9–26.9
HFC-143a	64.2	57.6–71.6
HFC-152a	1.8	1.3–2.3
CCl_4	47.0	30.0–58.0
CH_3CCl_3	6.1	5.0–7.2
CF_3Br	77.0	69.0–88.0

should give the correct history of the CO_2 concentration changes. Available estimates of CO_2 emissions and uptake by the ocean do not balance (IPCC, 1990), and this imbalance is generally attributed to the uncertainties in the uptake of CO_2 by the terrestrial biosphere and the ocean (IPCC, 1990, 1992; Tans *et al.*, 1990). The present uncertainties about these uptakes result from the lack of direct measurements of changes in the carbon content of the biosphere and the ocean. Therefore, we have to rely on model parameterizations to estimate oceanic and biospheric CO_2 uptake rates. Table II shows the CO_2 fluxes for recent years as well as their cumulative amounts from the pre-industrial time to 1990 as estimated by different models. The IPCC estimates are based on the simple steady-state models covering the period of 1980–1989. The Tans *et al.* (1990) estimates are based on their scenarios 5–8, which make use of a 3-D atmospheric transport model constrained by the interhemispheric gradient of CO_2 as estimated from observations for the period of 1980–1987. Siegenthaler and Oeschger (1987) as well as Siegenthaler and Joos (1992) have performed a deconvolution of the observed atmospheric CO_2 concentrations using a different version of the 1-D model. Sarmiento *et al.* (1992)

make use of a 3-D ocean carbon model. Various models listed in Table II yield an oceanic CO_2 uptake in recent years of between 0.3 and 3.3 GtC/yr. The low estimate, based on the evaluation of atmospheric CO_2 data and oceanic CO_2 using a 3-D atmospheric trace model, is inconsistent with the estimates of other ocean models reported in Table II. Sarmiento and Sundquist (1992) have revised the ocean sink estimates of Tans *et al.* (1990). According to their estimates, the revised net oceanic CO_2 uptake for the period 1980–1989 was 2.0 ± 0.8 GtC/yr which is in agreement with the IPCC and other model calculations. The high oceanic uptake of 3.3 GtC/yr is estimated with an outcrop-diffusion model which overestimates the flux into the ocean, because the exchange between the high-latitude surface waters and the deep ocean water is too fast. We, therefore, use the IPCC's lower (1.0 GtC/yr) and upper limit (3 GtC/yr) for modeling the oceanic uptake of CO_2. The last four columns in Table II present the same parameters for four cases as calculated with the carbon cycle model used in this study (and described in the next section).

3.1. MODEL DESCRIPTION

We have used a coupled climate carbon-cycle model described in Jain and Bach (1994) to calculate the decay rate for CO_2. This model contains a box-diffusion carbon cycle model consisting of three reservoirs, namely the atmosphere, the mixed ocean layer (ca. 75 m) and the deep ocean (ca. 3925 m). The model equations which describe the rate of change of carbon in each box are those taken from Oeschger *et al.* (1975). The model ocean is treated as a diffusion medium with constant vertical eddy diffusivity. The model also takes into account the interaction with the biosphere. The biospheric emissions are calculated by a multi-box globally aggregated terrestrial biosphere submodel developed by Harvey (1989), which distinguishes between ground vegetation, nonwoody tree parts, woody tree parts, detritus, and slowly and rapidly overturning soil carbon reservoirs. The biosphere model takes into account the biosphere respiration-temperature feedback. The one-dimensional upwelling-diffusion model of Harvey and Schneider (1985) is used to infer the surface temperature changes.

As discussed by IPCC (1990), the ocean flux is not sufficient for balancing the carbon budget. We therefore allow a terrestrial sink mainly due to CO_2 fertilization feedback to balance the carbon cycle model. Balance can be achieved for a range of oceanic flux and net terrestrial flux combinations. Thus, one can estimate the range of GWP values that correspond to the range of model parameters. We balance our carbon cycle model for the 1980s mean ocean flux F_{oc} (1980s) range 1–3 GtC/yr in combination with the net terrestrial uptake values which give the correct history of the CO_2 concentration. The main carbon cycle model parameters, including the values of adjustable parameters used in the four balanced carbon cycle cases, are given in Table III.

TABLE II

Anthropogenic perturbations of a CO_2 increase estimated by various models

	IPCC (1990)	Tans *et al.* (1990)[2]	Siegenthaler and Oeschger (1987)	Siegenthaler and Joos (1992)	Sarmiento *et al.* (1992)	Present Study		
						β: 0.215 K: 2.5×10^{-4}	0.400 1.3×10^{-4}	0.770 0.2×10^{-4}
Fluxes for period/ year (GtC/yr)	1980–1989	1980–1987	1980	1980	1980		1980–1990	
Industrial	5.4 ± 0.5	5.3	5.28	5.26	5.24	5.38	5.38	5.38
Deforestation	1.6 ± 1.0	0.0–3.2	–	–	–	1.80	1.80	1.80
Inferred terrestrial uptake	1.8 ± 1.4	2.0 ± 4.7	–	–	–	0.75	1.44	2.73
Net terrestrial uptake[1]	–0.2 ± 1.7	–(2.0–1.5) (–1.2–0.1)[3]	0.10–1.18	–0.22–0.09	–0.48	1.05	0.36	–0.93
Atmospheric increase	3.2 ± 0.1	3.0	3.13	3.11	3.09	3.44	3.44	3.44
Oceanic uptake	2.0 ± 0.8	0.3–0.8 (1.1–2.4)[3]	2.25–3.33	1.93–2.16	1.67	2.99	2.30	1.01
Perturbation for period (GtC)	1850–1990	–	1770–1980	1770–1980	1770–1780		1860–1990	
Fossil	200.0 ± 20	–	163	162	162	210	210	210
Deforestation	115 ± 35	–	–	–	–	118	118	118
Terrestrial uptake	–	–	–	–	–	38	69	–129
Net terrestrial uptake	–	–	88–153	72–88	56	80	49	–11
Atmospheric increase	–	–	128	127	127	155	155	155
Oceanic uptake	–	–	123–188	107–123	92	135	104	46

[1] Net terrestrial uptake = Deforestation-inferred terrestrial uptake.

[2] The total terrestrial and oceanic uptake is fixed at 2.3 GtC/yr in all their scenarios.

[3] Modified by Sarmiento and Sundquist (1992).

TABLE III

Values of fixed and adjustable parameters for carbon cycle model

Fixed parameters			
CO_2 concentration in pre-industrial atmosphere	282 ppm		
CO_2 mass in pre-industrial atmosphere	598 GtC		
CO_2 mass in pre-industrial mixed layer	669 GtC		
Carbon concentration in pre-industrial atmosphere	2.05 mol m^{-3}		
CO_2 biospheric mass in pre-industrial ocean	2327 GtC		
^{14}C concentration in pre-industrial atmosphere	1		
^{14}C concentration in pre-industrial mixed layer	0.95		
^{14}C concentration in pre-industrial deep ocean	0.84		
Average depth of the mixed layer	75 m		
Average depth of the deep ocean	3725 m		
Thickness of the ocean layer containing as much carbon as pre-industrial atmosphere (for 598 GtC)	67 m		
Ocean surface area	3.62×10^{14} m^2		
Buffer factor for excess CO_2	9		
Decay constant of ^{14}C	1/8267 yr		
Adjustable parameters			
CO_2 fertilization factor (β factor)	0.2	0.4	0.8
Eddy diffusivity (m^2 s^{-1})	2.5×10^{-4}	1.3×10^{-4}	0.2×10^{-4}
Exchange coefficient			
– atmosphere to mixed layer (yr^{-1})	0.122	0.115	0.063
– mixed layer to atmosphere (yr^{-1})	0.109	0.103	0.056

In our box diffusion model, the ocean flux is controlled by the effective eddy diffusive coefficient 'K' to change the rate of CO_2 uptake. Regarding the terrestrial biospheric component of the carbon cycle model, there are three feedbacks: (i) direct stimulation of photosynthesis and carbon storage by higher atmospheric CO_2 concentration (CO_2 fertilization effect); (ii) stimulation of photosynthesis and carbon storage by warmer temperature; and (iii) enhanced respiration by plants, detritus, and soil carbon due to warmer temperature. The first two feedbacks are negative (tending to reduce the CO_2 increase), while the third feedback is positive (tending to increase atmospheric CO_2). The most important of these is the negative feedback due to CO_2 fertilization which is controlled by the fertilization factor β. Table II shows the combination of β and K values giving results which are close to the observed CO_2 concentrations from 1860 to 1990.

The effective eddy diffusivity K is determined by the method of Oeschger *et al.* (1975) in such a way that the ^{14}C concentration in the pre-industrial mixed

layer and the deep ocean are 0.95 and 0.84, respectively. The most probable value of K for a box diffusion model is 1.27×10^{-4} m^2 s^{-1} (Oeschger *et al.*, 1975; Siegenthaler, 1983). Once K is known the exchange coefficients can be calculated from the Equation 19 of Oeschger *et al.* (1975). The resulting exchange coefficient values corresponding to $K = 1.27 \times 10^{-4}$ m^2 s^{-1} are 0.12 per yr (atmosphere to mixed layer) and 0.10 per year (mixed layer to atmosphere), respectively. Previous studies have suggested that a β value from 0.2 to 0.8 is necessary to simulate the observed atmospheric CO_2 concentration (Kohlmaier *et al.*, 1987, 1989; Gates, 1985). $\beta = 0.4$ is currently considered as the most likely estimate (Bacastow and Keeling, 1973; Goudriaan and Ketner, 1984; Harvey, 1989; Kohlmaier *et al.*, 1991). For the middle guess case ($K = 1.27 \times 10^{-4}$ m^2 s^{-1} and $\beta = 0.4$), our model-estimated value of oceanic CO_2 uptake for the decade 1980–1990 (F_{oc}(1980s)) is 2.3 GtC/yr which is in close agreeement with the other model estimates shown in Table II. Quay *et al.* (1992) have also estimated the same amount of CO_2 uptake for the period 1970–1990. The 3-D model of Sarmiento *et al.* (1992) yields less oceanic uptake than the simple models shown in Table II. This is due to the fact that their model ocean has an uptake of bomb ^{14}C into the thermocline that is too small. In addition to the reference case, we also balance the model for two extreme cases F_{oc}(1980s) = 1.0 and 3.0 GtC/yr using the pairs of values of β (0.770 and 0.215) and K (0.2×10^{-4} and 2.5×10^{-4} m^2 s^{-1}) shown in Table II. The diffusion coefficient obtained with the box diffusion model for F_{oc}(1980s) = 1 GtC/yr turned out to be only 1.58×10^{-5} m^2 s^{-1}, which is very low but still higher than those determined for actual vertical mixing in limited areas, typically 9.51×10^{-6} m^2 s^{-1} and less (Gargett, 1976; Jenkins, 1980). It should be emphasized, however, that eddy diffusion in a global model is a concept summarizing quite different physical mixing and transport processes and can therefore not be compared directly with the turbulent diffusion on a local scale.

3.2. PAST CO_2 EMISSIONS

For each of the three cases, the carbon cycle model was run from 1860 to 1990 using industrial (fossil fuel burning and cement production) and land use CO_2 emissions data which is taken from Keeling (1973), Rotty (1987) and Boden *et al.* (1991) (see Figure 1). The mean CO_2 flux from fossil fuels and cement production for the decade 1980–1990 is 5.38 GtC/yr. The estimated cumulative emission of CO_2 from these sources from 1860 to 1990 is 210 GtC. Table II shows that our estimates are in good agreement with that of IPCC (1990) and other published analyses. For the CO_2 emissions from land use changes for the period of 1860–1980, we have used the Harvey (1989) low estimate, which in turn was originally derived from the emissions curve for 1860–1990 in Figure 8 of Houghton *et al.* (1983). The estimated land use emission in 1980 was 1 GtC/yr as compared to the IPCC (1990) estimate of 0.6–2.5 GtC. Recent analysis of current land use changes in tropical regions and in the temperate and borel regions were combined to yield a global

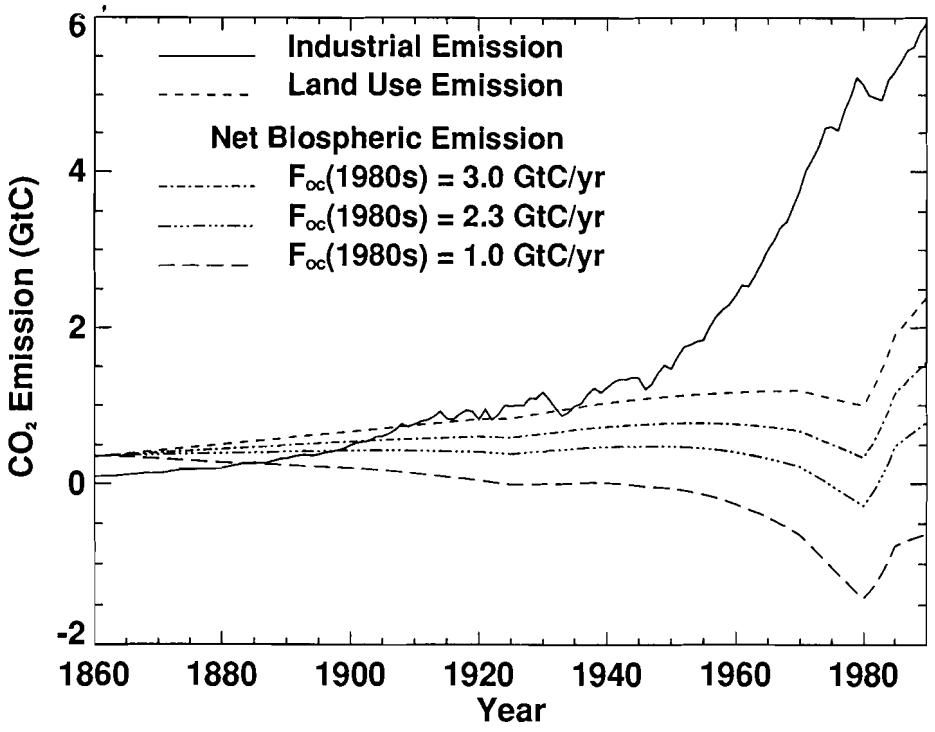

Fig. 1. Industrial and land use emissions of CO_2 from 1860 to 1990 used in this study. Also shown is the net terrestrial emissions calculated for various experiments (F_{oc}(1980s) = 1.0, 2.3, and 3.0 GtC/yr.)

estimate of 1.1–3.6 GtC in 1990 (Houghton, 1991). The midpoint of the range is 2.35 GtC. In this paper, the carbon emission due to land use changes is assumed to increase exponentially from 1 to 2.35 GtC between 1980 and 1990 (Figure 1). This substantial increase of carbon emission is consistent with the recent figures of deforested area which show that the area deforested in 1990 was 50% (FAO, 1990, 1991) to 90% (Myers, 1991) higher than the area deforested in 1980. The estimated CO_2 emissions from land use changes for the decade 1980–1990 and for the period 1860–1990 were 1.8 GtC/yr and 118 GtC, which are consistent with the IPCC (1990) values within their uncertainty limits.

Figure 1 also shows the net terrestrial biospheric emissions ($B(t)$) (Land use emissions-inferred terrestrial uptake) for β ranging from 0.2 to 0.8 for the period 1860–1990. The curves for $B(t)$ show a close resemblance to those obtained by Siegenthaler and Oeschger (1987), Siegenthaler and Joos (1992), and Sarmiento *et al.* (1992) who estimated $B(t)$ using different models. Figure 1 suggests that the biospheric emission, $B(t)$, was larger than the industrial emission in the 19th century, while in the 20th century continued industrialization has led to a dramatic increase in fossil fuel emissions. For the F_{oc}(1980s) = 2.3 and 3.0 curves, a slow

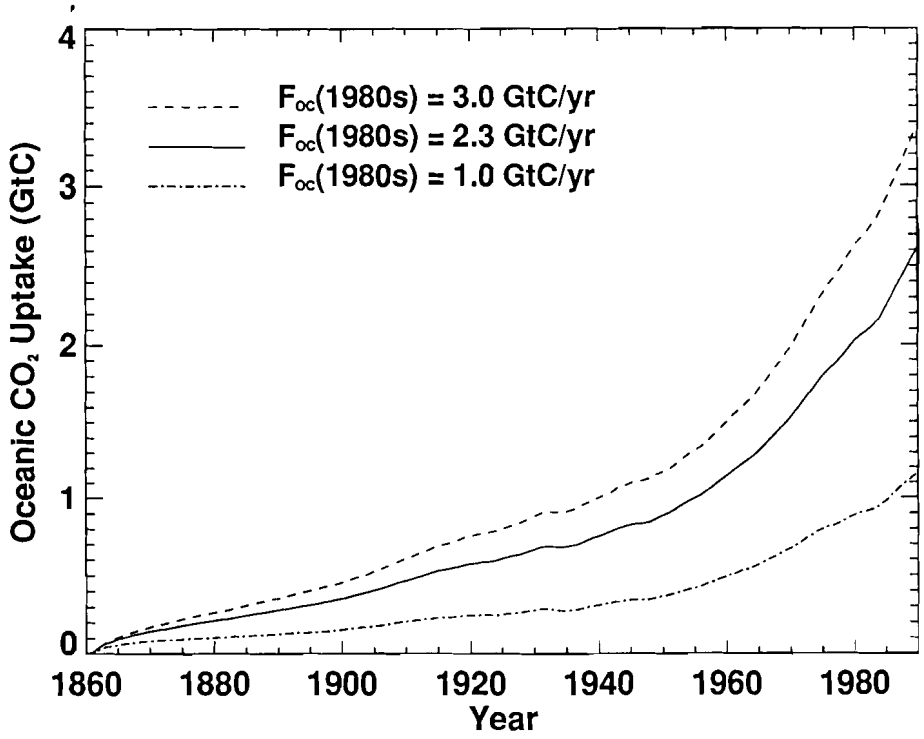

Fig. 2. Net oceanic CO_2 uptake for the various experiments from 1860 to 1990.

increase of $B(t)$ occurs up to the 1960s, followed by a decline and then a rapid increase starting in the late 1970s. The rapid increase in the late 1970s obtained here is also evident in the recently published deconvolution calculation of $B(t)$ by Siegenthaler and Joos (1992). Note that the low ocean flux (F_{oc}(1980s) = 1.0 GtC) lead to a much larger imbalance (B(1980s) = −1.0 GtC/yr) but are still within the range of uncertainties. For the F_{oc}(1980s) range of 3.0 (2.3) 1.0 (bracketed value is the reference value), the model estimated net terrestrial uptake for the decade 1980–1990 was +1.0 (+0.4) −0.1; these values compare well with other published evaluations (see Table II). The estimated total net terrestrial CO_2 uptake between 1860 and 1990 was 80 (49) 11 GtC. Our best estimate of 49 GtC is in close agreement with that obtained from the 3-D model of Sarmiento *et al.* (1992) (ca. 56 GtC from 1770 to 1980). Figure 2 shows the net oceanic uptake for various cases from 1860 to 1990. It is clearly evident from Figure 1 and Figure 2 that the larger ocean flux requires smaller terrestrial uptake and vice versa to balance the carbon budget.

3.3. PAST CO_2 CONCENTRATIONS

Figure 3 shows the computed atmospheric CO_2 concentration along with the observed atmospheric concentrations from 1860 to 1990. The observed CO_2 data from 1860 to 1957 are obtained from the Siple ice-core, measured by infrared laser spectroscopy (Friedli *et al.*, 1986) and thereafter from Mauna Loa Observatory, Hawaii, which is representative of the global mean (Keeling *et al.*, 1989). It is seen that the carbon cycle model with biospheric feedbacks (i.e. balanced case) gives a slight underestimation in the 19th century and earlier 20th century, as compared to the observed data. In general, the model is capable of reproducing satisfactorily the observed concentration trends. Excluding the effects of the biosphere (i.e. unbalanced case), from 1860 to 1990, results in an over-estimation of CO_2 concentration, ca. 6% as compared to the balanced case. The pre-industrial CO_2 concentration appears to have ranged between 280 and 285 ppm (Gammon *et al.*, 1985; Oeschger and Stauffer, 1986). In the present study, we take 282 ppm as the starting concentration for all the cases. In 1990, modelled atmospheric CO_2 concentration (ppm) for the balanced cases was 354.0 ppm compared to the observed concentration of 353.8 (IPCC, 1990). Therefore, the atmospheric increases in CO_2 concentration calculated for each of the balanced carbon cycle cases during the decade 1980 to 1990 and for the period 1860 to 1990 are 1.6 ppm/yr (3.4 GtC/yr) and 72 ppm (155 GtC), respectively (as indicated in Table II).

3.4. MODEL RESPONSE TO A PULSE CO_2 INPUT

A key element in the determination of GWPs is the changing atmospheric lifetime of CO_2 in the atmosphere; in the carbon cycle model this is characterized by the response to a pulse input of excess CO_2 into the atmosphere. We consider five future background emission scenarios for CO_2: constant concentrations at the 1990 level of 354 ppm, constant emissions at the 1990 level of 7.4 C/yr (industrial plus net land use) and three of the IPCC emission scenarios (two extreme cases and one intermediate case), IS92a, IS92c, and IS92e (IPCC, 1992).

In all the experiments the model was initialized to a 282 ppmv steady-state at the year 1860. The model was then run from 1860 to 1990, with the specified total CO_2 emissions. From 1990 onwards, the model was run with the prescribed background emission scenario both with and without an additional 1 GtC pulse injected into the 1990 disequilibrium atmosphere. Figure 4 shows the impulse response curves derived for different F_{oc}(1980s) values for the constant concentration background scenario. Also shown in Figure 4 is the impulse response curve which was used in the prior IPCC studies, based on the unbalanced Siegenthaler and Oeschger (1987) carbon cycle model. It is important to note the differences between the balanced impulse response curves from this study and the IPCC curve. Figure 4 shows that the decay rate of atmospheric CO_2 is much faster for the balanced carbon cycle cases (F_{oc}(1980s) = 1.0, 2.3, and 3.0 GtC) during the first fifty years or more

3.3. PAST CO_2 CONCENTRATIONS

Figure 3 shows the computed atmospheric CO_2 concentration along with the observed atmospheric concentrations from 1860 to 1990. The observed CO_2 data from 1860 to 1957 are obtained from the Siple ice-core, measured by infrared laser spectroscopy (Friedli *et al.*, 1986) and thereafter from Mauna Loa Observatory, Hawaii, which is representative of the global mean (Keeling *et al.*, 1989). It is seen that the carbon cycle model with biospheric feedbacks (i.e. balanced case) gives a slight underestimation in the 19th century and earlier 20th century, as compared to the observed data. In general, the model is capable of reproducing satisfactorily the observed concentration trends. Excluding the effects of the biosphere (i.e. unbalanced case), from 1860 to 1990, results in an over-estimation of CO_2 concentration, ca. 6% as compared to the balanced case. The pre-industrial CO_2 concentration appears to have ranged between 280 and 285 ppm (Gammon *et al.*, 1985; Oeschger and Stauffer, 1986). In the present study, we take 282 ppm as the starting concentration for all the cases. In 1990, modelled atmospheric CO_2 concentration (ppm) for the balanced cases was 354.0 ppm compared to the observed concentration of 353.8 (IPCC, 1990). Therefore, the atmospheric increases in CO_2 concentration calculated for each of the balanced carbon cycle cases during the decade 1980 to 1990 and for the period 1860 to 1990 are 1.6 ppm/yr (3.4 GtC/yr) and 72 ppm (155 GtC), respectively (as indicated in Table II).

3.4. MODEL RESPONSE TO A PULSE CO_2 INPUT

A key element in the determination of GWPs is the changing atmospheric lifetime of CO_2 in the atmosphere; in the carbon cycle model this is characterized by the response to a pulse input of excess CO_2 into the atmosphere. We consider five future background emission scenarios for CO_2: constant concentrations at the 1990 level of 354 ppm, constant emissions at the 1990 level of 7.4 C/yr (industrial plus net land use) and three of the IPCC emission scenarios (two extreme cases and one intermediate case), IS92a, IS92c, and IS92e (IPCC, 1992).

In all the experiments the model was initialized to a 282 ppmv steady-state at the year 1860. The model was then run from 1860 to 1990, with the specified total CO_2 emissions. From 1990 onwards, the model was run with the prescribed background emission scenario both with and without an additional 1 GtC pulse injected into the 1990 disequilibrium atmosphere. Figure 4 shows the impulse response curves derived for different F_{oc}(1980s) values for the constant concentration background scenario. Also shown in Figure 4 is the impulse response curve which was used in the prior IPCC studies, based on the unbalanced Siegenthaler and Oeschger (1987) carbon cycle model. It is important to note the differences between the balanced impulse response curves from this study and the IPCC curve. Figure 4 shows that the decay rate of atmospheric CO_2 is much faster for the balanced carbon cycle cases (F_{oc}(1980s) = 1.0, 2.3, and 3.0 GtC) during the first fifty years or more

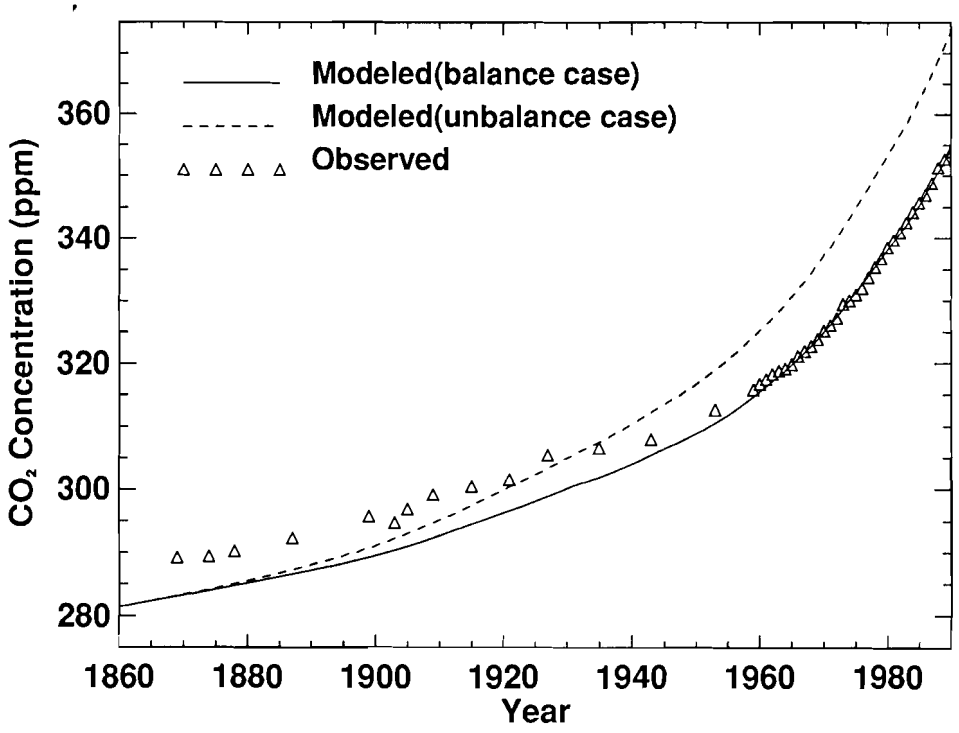

Fig. 3. Model-computed CO_2 concentration (with and without biospheric feedbacks), and observed CO_2 concentration, 1860–1990.

than for the unbalanced model cases, obviously because the biospheric feedbacks withdraw more CO_2 from the atmosphere which produce an enhanced short term decay. The decay rates for the balanced cases at later times depend on the specific assumptions used for the ocean flux and fertilizations factor. The reference case, corresponding to $F_{oc}(1980s) = 2.3$ GtC, decays more rapidly than the IPCC case for the first 150 years, and has a similar, but slightly slower, decay rate thereafter. Our model estimated ocean-only response (unbalanced case) is slightly slower than the IPCC curve for the first 100 years, but thereafter the response of the two unbalanced-case curves is quite similar.

4. Effect of Balancing the Carbon Budget

Table IVa presents equilibrium GWPs reproduced in IPCC (1992). These values are derived using the IPCC unbalanced carbon cycle model with a constant background CO_2 concentration scenario. The GWPs for the current unbalanced version of the model are also given in Table IVb. Our unbalanced model estimated GWP values are considerably lower for all time horizons compared to IPCC GWPs because the

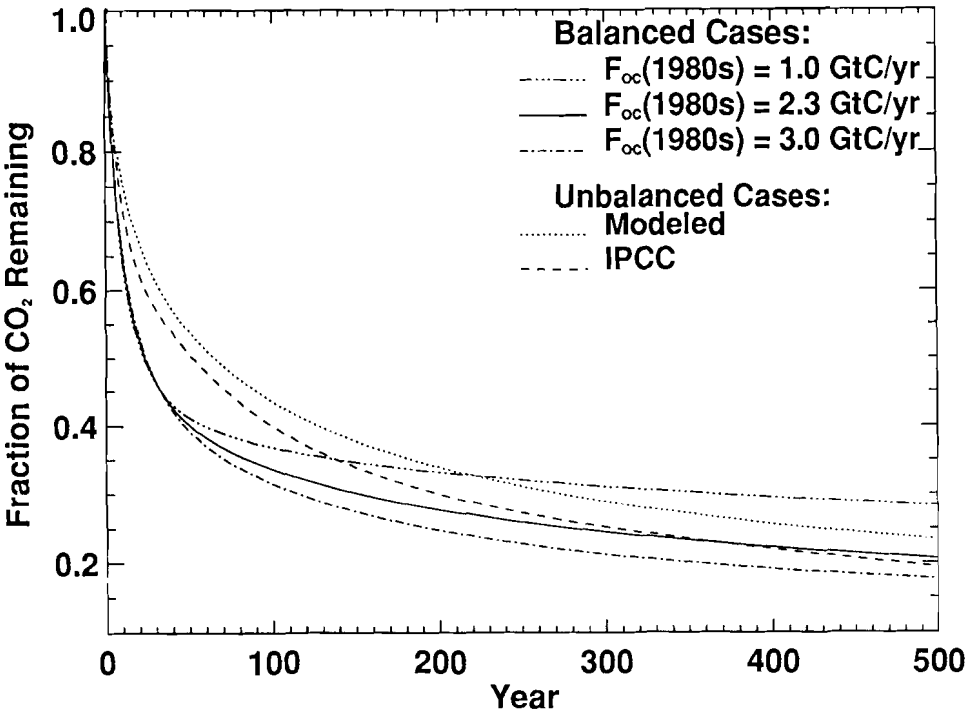

Fig. 4. Model response of atmospheric CO_2 to a pulse input of 1 GtC for constant background concentration scenario. For the best guess case ($\beta = 0.4$ and $K = 1.27 \times 10^{-4}$ m^2 s^{-1}), F_{oc}(1980s) is 2.3 GtC/yr. Other balanced carbon cycle cases ($\beta = 0.2$, 0.8 and $K = 2.51 \times 10^{-4}$, 0.16×10^{-4} m^2 s^{-1}), F_{oc}(1980s) of 3.0, and 1.0 GtC/yr curves, consider the range of uncertainties associated with the treatment of ocean and terrestrial biosphere processes in determining a balanced carbon cycle. The IPCC curve is based on the Siegenthaler and Oeschger (1987) carbon cycle model as used in the IPCC evaluations of Global Warming Potentials.

ocean response of the unbalanced version of the current model is slower than that of the IPCC unbalanced model. The difference amounts to 3% at $T = 20$ yr to 12% at $T = 500$ yr.

To obtain further insight into the uncertainties in IPCC GWPs, we compare the current balanced carbon cycle model GWPs with IPCC GWPs. Equilibrium GWPs derived for the constant-concentration impulse response functions with F_{oc}(1980s) = 2.3 GtC/yr and $\beta = 0.4$ are given in Table V. The difference between these GWPs and the IPCC GWPs (Table IVa) is in the integrated radiative forcing of CO_2 arising from the balanced carbon cycle model compared with that from the IPCC unbalanced model. Percentage differences between the three balanced cases and the IPCC GWPs are given in Table VI; since the balanced carbon cycle effect only changes the integrated radiative forcing of CO_2, the difference does not depend on the identity of the trace gas (note that the GWP for CO_2 is always unity by definition; the factors shown apply to other trace gases). The rapid CO_2 decay

in the 'reference' case ($\beta = 0.4$, $F_{oc}(1980s) = 2.3$ GtC/yr) compared with the IPCC unbalanced model causes a systematic enhancement in GWPs at short time horizons T: 10% for $T = 20$ yr which increases to 19% at $T = 100$ yr. As time proceeds, however, the two impulse response functions converge, and the balanced carbon cycle response function is only slightly larger than the IPCC function for times exceeding 400 yr (Figure 4).

As seen in Table VI, the choice of combination of biological feedback β and ocean uptake rate $F_{oc}(1980s)$ produce a considerable effect on GWPs defined for a balanced carbon cycle. It is important to note that the larger β (or smaller $F_{oc}(1980s)$ gives smaller GWPs (Table VI) because the biospheric uptake of CO_2 saturates faster than the oceanic uptake for a larger β, resulting in a larger CO_2 concentration with an increasing time horizon and hence smaller GWPs. The range of the derived GWPs provides an estimate of the uncertainties associated with current capabilities for deriving a balanced carbon cycle. For $\beta = 0.8$, the enhancement at $T = 20$ yr is 10% due to the fast initial decay of CO_2. However, in order to balance this scenario, the smaller ocean uptake $F_{oc}(1980s) = 1.0$ GtC/yr is required and the resulting impulse response function exhibits a considerably slower decay than the IPCC function for times beyond 150 yr, with the two functions crossing over before $T = 150$ yr (Figure 4). The GWP enhancement of 17% at $T = 100$ yr thus becomes 9% at $T = 200$ yr, then –7% at $T = 500$ yr. The balanced scenario with $\beta = 0.2$ and $F_{oc}(1980s) = 3.0$ GtC/yr has a long-term decay that is somewhat greater than that of the reference case $\beta = 0.4$ (Figure 4). Accordingly, for this case the GWPs are greater than the IPCC GWPs for all time horizons, varying from 9% at $T = 20$ yr to 22% at $T = 200$ yr, then 20% at $T = 500$ yr. An examination of all of the cases for the balanced carbon cycle indicate that the GWPs are least uncertain at $T = 20$ yr and become more uncertain with increasing T, up to the range of –7 to +20% at $T = 500$ yr.

5. Effect of Carbon Cycle Nonlinearities

As the emission rate of CO_2 into the atmosphere varies in the future, there are two resulting effects on GWPs that need to be considered. First, carbon cycle nonlinearities result because the response to a pulse input in 1990 is expected to depend not only on the past emissions but also on future emissions. Secondly, radiative forcing nonlinearities result because the radiative forcing due to CO_2 varies nonlinearly with CO_2 concentration, so that the CO_2 integrated radiative forcing (and therefore GWPs) should vary nonlinearly with the CO_2 concentration resulting from a given emission scenario. In this section, we examine the response of derived GWPs to the first effect.

In order to estimate the effect of changes in the future background atmosphere, we consider four CO_2-emission background scenarios, a constant-emission and three scenarios from the recent IPCC report (IPCC, 1992), as noted above. The

TABLE IV

Equilibrium GWPs derived for CO_2-constant concentration scenario with (a) IPCC (1992) unbalanced carbon cycle model; and (b) unbalanced version of the current carbon cycle model

	(a) GWP at time horizon (years)				
Gas	20	50	100	200	500
CO_2	1.0	1.0	1.0	1.0	1.0
CH_4	34.3	18.9	11.2	6.9	3.8
N_2O	254.0	269.0	266.0	239.0	165.0
CFC-11	4420.0	4100.0	3370.0	2400.0	1360.0
CFC-12	7010.0	7330.0	7090.0	6180.0	4100.0
HCFC-22	4090.0	2580.0	1580.0	968.0	535.0
CFC-113	4490.0	4670.0	4480.0	3850.0	2510.0
CFC-114	5960.0	6600.0	6950.0	6960.0	5780.0
CFC-115	5390.0	6210.0	6970.0	7820.0	8460.0
HCFC-123	332.0	157.0	92.1	56.4	31.2
HCFC-124	1540.0	776.0	455.0	279.0	154.0
HFC-125	5150.0	4430.0	3350.0	2230.0	1240.0
HFC-134a	3080.0	1940.0	1180.0	725.0	401.0
HCFC-141b	1810.0	1020.0	608.0	372.0	206.0
HCFC-142b	3930.0	2820.0	1830.0	1140.0	628.0
HFC-143a	4670.0	4470.0	3820.0	2830.0	1640.0
HFC-152a	524.0	248.0	145.0	89.0	49.1
CCl_4	1770.0	1580.0	1250.0	854.0	478.0
CH_3CCl_3	351.0	173.0	101.0	62.0	34.2
CF_3Br	5530.0	5460.0	4880.0	3800.0	2270.0
	(b) GWP at time horizon (years)				
Gas	20	50	100	200	500
CO_2	1.0	1.0	1.0	1.0	1.0
CH_4	33.2	18.0	10.5	6.3	3.4
N_2O	244.7	255.4	250.1	221.0	148.3
CFC-11	4271.7	3893.4	3175.2	2219.8	1221.2
CFC-12	6767.3	6962.7	6678.0	5712.9	3674.6
HCFC-22	3948.6	2451.0	1485.0	894.8	479.3
CFC-113	4337.8	4434.9	4214.6	3556.3	2250.1
CFC-114	5754.3	6264.2	6542.8	6433.3	5177.0
CFC-115	5206.4	5895.5	6556.6	7231.8	7588.0
HCFC-123	321.0	149.3	86.8	52.2	28.0
HCFC-124	1489.3	736.4	428.5	257.7	138.1
HFC-125	4970.4	4208.05	3158.0	2060.3	1111.7
HFC-134a	2976.9	1839.5	1112.7	670.4	359.1
HCFC-141b	1749.1	972.0	572.1	344.1	184.4
HCFC-142b	3790.0	2674.0	1724.9	1049.9	562.5
HFC-143a	4508.4	4240.5	3596.5	2618.9	1467.4
HFC-152a	506.3	235.6	137.0	82.4	44.1
CCl_4	1704.8	1498.9	1172.1	789.0	428.7
CH_3CCl_3	338.8	163.8	95.2	57.3	30.7
CF_3Br	5340.0	5188.3	4591.7	3515.7	2031.7

TABLE V

Equilibrium GWPs for CO_2-constant concentration scenarios with the balanced carbon cycle model using the reference 1980s-mean oceanic uptake $F_{oc}(1980s) = 2.3$ GtC/yr and fertilization factor $\beta = 0.4$

	GWP at time horizon (years)				
Gas	20	50	100	200	500
CO_2	1.0	1.0	1.0	1.0	1.0
CH_4	37.7	22.1	13.4	8.0	4.1
N_2O	278.0	314.0	317.0	279.0	181.0
CFC-11	4860.0	4790.0	4020.0	2800.0	1490.0
CFC-12	7690.0	8570.0	8460.0	7210.0	4480.0
HCFC-22	4490.0	3020.0	1880.0	1130.0	584.0
CFC-113	4930.0	5460.0	5340.0	4490.0	2740.0
CFC-114	6550.0	7710.0	8290.0	8130.0	6310.0
CFC-115	5920.0	7260.0	8310.0	9140.0	9250.0
HCFC-123	365.0	184.0	110.0	66.0	34.1
HCFC-124	1690.0	907.0	543.0	326.0	168.0
HFC-125	5650.0	5180.0	4000.0	2600.0	1350.0
HFC-134a	3390.0	2260.0	1410.0	847.0	438.0
HCFC-141b	1990.0	1200.0	725.0	435.0	225.0
HCFC-142b	4310.0	3290.0	2190.0	1330.0	686.0
HFC-143a	5130.0	5220.0	4560.0	3310.0	1790.0
HFC-152a	576.0	290.0	174.0	104.0	53.8
CCl_4	1940.0	1840.0	1490.0	997.0	522.0
CH_3CCl_3	385.0	202.0	121.0	72.4	37.4
CF_3Br	6070.0	6390.0	5820.0	4440.0	2480.0

TABLE VI

Percent difference in equilibrium GWPs for three balanced carbon cycle cases compared with IPCC (1992) calculations

$F_{oc}(1980s)$/ GtC yr^{-1}	β	Percent difference in GWPs at Time Horizon/yr				
		20	50	100	200	500
3.0	0.2	8.9	16.6	21.3	22.2	19.7
2.3	**0.4**	**9.8**	**16.9**	**19.3**	**16.8**	**9.2**
1.0	0.8	10.9	17.2	16.6	8.8	−7.2

chosen IPCC emission scenarios represent the intermediate case (Scenario IS92a), the lower extreme case in CO_2 emissions (Scenario IS92c, which is nearly similar to the constant-emission case), and the upper extreme (Scenario IS92e). Figures 5a and 5b show the emissions and model-derived concentrations for all IPCC six scenarios from 1990 to 2100. The balanced version of the carbon cycle is used to calculate concentrations of CO_2 using the reference values of fertilization parameter $\beta = 0.4$ and 1980s ocean flux $F_{oc}(1980s) = 2.3$ GtC/yr. To estimate the impulse response curves to 500 yr, emissions in these scenarios are assumed to remain constant after 2100. Figure 6 shows that the IPCC (1992) impulse response functions derived for these scenarios are quite similar, showing that the carbon cycle nonlinearities are small in our model.

These results suggest that derived GWPs should also have a minor dependence on the impulse response function from the various scenarios. For each derived impulse response function, equilibrium GWPs are calculated and compared with those of the constant-emission case (Table VIIa). The equilibrium GWPs for the IPCC (1992) scenarios are given in Tables VIIb, c, and d. Percentage differences in GWP between three of the IPCC scenarios and those of the constant-emission best case are shown in Table VIII. At time horizons from 20 to 50 years, the differences among the GWPs for the three emission scenarios are insignificant at less than one percent, but vary from the constant-emissions case by roughly one percent. The equilibrium GWPs produced by the IPCC low scenario IS92c are about 3% greater than those of the constant-emission case at 500 year due to the slightly lower values of the impulse response function (Figure 6). For scenarios IS92a and IS92e, however, slightly slower decay in the impulse response functions compared to Scenario IS92c occur (Figure 6) past time horizons of 50 yr, and a significant decrease in GWPs begins at 100 yr. At a time horizon of 500 yr, the impulse response function for the high CO_2 emissions scenario results in values 4.7% larger than the constant-emissions case, while the low emissions scenario results in values 2.7% smaller than the constant emissions case. Overall, the effect of emissions scenario on derived GWPs through the impulse response function for CO_2 is generally less significant in comparison to the magnitude of other uncertainties examined in this study.

6. Effect of Radiative Forcing Nonlinearities

The change in radiative forcing associated with a small impulse of CO_2 is inversely proportional to the concentration of CO_2 (IPCC, 1990). Where atmospheric CO_2 concentrations increase with time, integrated CO_2 radiative forcing should be smaller for the disequilibrium than for equilibrium case, and resulting GWPs for gases other than CO_2 should be larger. Table IX lists the GWP values resulting for disequilibrium CO_2 concentrations following the constant-emission scenario and the three IPCC emission scenarios (IS92e, IS92a, IS92c). Percentage enhancements

TABLE VII

Equilibrium GWPs derived for constant-emission and three IPCC (1992) CO_2 emission scenarios with the balance carbon cycle model using reference values of F_{oc} (1980s) = 2.3 GtC/yr and $\beta = 0.4$

(a) Constant-emission scenario GWPs at time horizon (years)					
Gas	20	50	100	200	500
CO_2	1.0	1.0	1.0	1.0	1.0
CH_4	37.7	21.7	12.9	7.5	3.8
N_2O	278.0	309.0	306.0	263.0	167.0
CFC-11	4860.0	4710.0	3880.0	2640.0	1370.0
CFC-12	7700.0	8410.0	8160.0	6800.0	4140.0
HCFC-22	4490.0	2960.0	1810.0	1060.0	540.0
CFC-113	4930.0	5360.0	5150.0	4230.0	2530.0
CFC-114	6540.0	7570.0	7990.0	7650.0	5830.0
CFC-115	5920.0	7120.0	8010.0	8600.0	8540.0
HCFC-123	360.0	180.0	106.0	62.0	31.4
HCFC-124	1690.0	890.0	523.0	307.0	155.0
HFC-125	5650.0	5090.0	3860.0	2450.0	1250.0
HFC-134a	3390.0	2220.0	1360.0	797.0	404.0
HCFC-141b	1990.0	1170.0	699.0	409.0	208.0
HCFC-142b	4310.0	3230.0	2110.0	1250.0	633.0
HFC-143a	5130.0	5120.0	4390.0	3120.0	1650.0
HFC-152a	575.0	284.0	167.0	97.8	49.6
CCl_4	1940.0	1810.0	1430.0	939.0	483.0
CH_3CCl_3	385.0	200.0	120.0	68.1	34.5
CF_3Br	6070.0	6270.0	5610.0	4180.0	2290.0
(b) IPCC Scenario IS92e (High) GWPs at time horizon (years)					
Gas	20	50	100	200	500
CO_2	1.0	1.0	1.0	1.0	1.0
CH_4	38.0	21.9	12.8	7.3	3.6
N_2O	280.0	311.0	304.0	255.0	159.0
CFC-11	4890.0	4740.0	3860.0	2560.0	1310.0
CFC-12	7750.0	8480.0	8110.0	6590.0	3940.0
HCFC-22	4520.0	2980.0	1800.0	1030.0	515.0
CFC-113	4970.0	5400.0	5120.0	4100.0	2420.0
CFC-114	6590.0	7620.0	7950.0	7420.0	5560.0
CFC-115	5960.0	7180.0	7970.0	8340.0	8140.0
HCFC-123	367.0	182.0	105.0	60.1	30.0
HCFC-124	1710.0	896.0	521.0	297.0	148.0
HFC-125	5690.0	5120.0	3840.0	2380.0	1190.0
HFC-134a	3410.0	2240.0	1350.0	773.0	386.0
HCFC-141b	2000.0	1180.0	695.0	397.0	198.0
HCFC-142b	4340.0	3260.0	2100.0	1210.0	604.0
HFC-143a	5160.0	5160.0	4370.0	3020.0	1580.0
HFC-152a	579.0	286.0	166.0	94.8	47.3
CCl_4	1950.0	1820.0	1420.0	910.0	460.0
CH_3CCl_3	388.0	199.0	116.0	66.0	32.9
CF_3Br	6120.0	6320.0	5580.0	4050.0	2180.0

TABLE VII

(continued)

(c) IPCC Scenario IS92a (Intermediate) GWPs at time horizon (years)					
Gas	20	50	100	200	500
CO_2	1.0	1.0	1.0	1.0	1.0
CH_4	38.0	21.9	12.9	7.4	3.7
N_2O	280.0	312.0	307.0	260.0	162.0
CFC-11	4890.0	4750.0	3890.0	2610.0	1330.0
CFC-12	7750.0	8490.0	8180.0	6710.0	4020.0
HCFC-22	4520.0	2990.0	1820.0	1050.0	524.0
CFC-113	4970.0	5410.0	5170.0	4180.0	2460.0
CFC-114	6590.0	7640.0	8020.0	7560.0	5660.0
CFC-115	5960.0	7190.0	8040.0	8500.0	8290.0
HCFC-123	367.0	182.0	106.0	61.2	30.5
HCFC-124	1710.0	898.0	525.0	303.0	151.0
HFC-125	5690.0	5130.0	3870.0	2420.0	1220.0
HFC-134a	3410.0	2240.0	1360.0	788.0	393.0
HCFC-141b	2000.0	1190.0	701.0	404.0	202.0
HCFC-142b	4340.0	3260.0	2110.0	1230.0	615.0
HFC-143a	5160.0	5170.0	4410.0	3080.0	1600.0
HFC-152a	579.0	287.0	168.0	96.6	48.2
CCl_4	1950.0	1830.0	1440.0	927.0	469.0
CH_3CCl_3	388.0	200.0	117.0	67.3	33.5
CF_3Br	6120.0	6330.0	5630.0	4130.0	2220.0

(d) IPCC Scenario IS92c (Low) GWPs at time horizon (years)					
Gas	20	50	100	200	500
CO_2	1.0	1.0	1.0	1.0	1.0
CH_4	38.0	22.0	13.1	7.7	3.9
N_2O	280.0	312.0	310.0	269.0	171.0
CFC-11	4890.0	4760.0	3940.0	2700.0	1410.0
CFC-12	7750.0	8520.0	8290.0	6960.0	4250.0
HCFC-22	4520.0	3000.0	1840.0	1090.0	554.0
CFC-113	4970.0	5430.0	5230.0	4330.0	2600.0
CFC-114	6590.0	7660.0	8120.0	7840.0	5980.0
CFC-115	5960.0	7210.0	8140.0	8810.0	8770.0
HCFC-123	367.0	182.0	108.0	63.5	32.3
HCFC-124	1710.0	901.0	532.0	314.0	160.0
HFC-125	5690.0	5150.0	3920.0	2510.0	1280.0
HFC-134a	3410.0	2250.0	1380.0	817.0	415.0
HCFC-141b	2000.0	1190.0	710.0	419.0	213.0
HCFC-142b	4340.0	3270.0	2140.0	1280.0	650.0
HFC-143a	5160.0	5190.0	4460.0	3190.0	1700.0
HFC-152a	579.0	288.0	170.0	100.0	50.9
CCl_4	1950.0	1830.0	1450.0	961.0	496.0
CH_3CCl_3	388.0	198.0	116.0	69.8	35.5
CF_3Br	6120.0	6350.0	5700.0	4280.0	2350.0

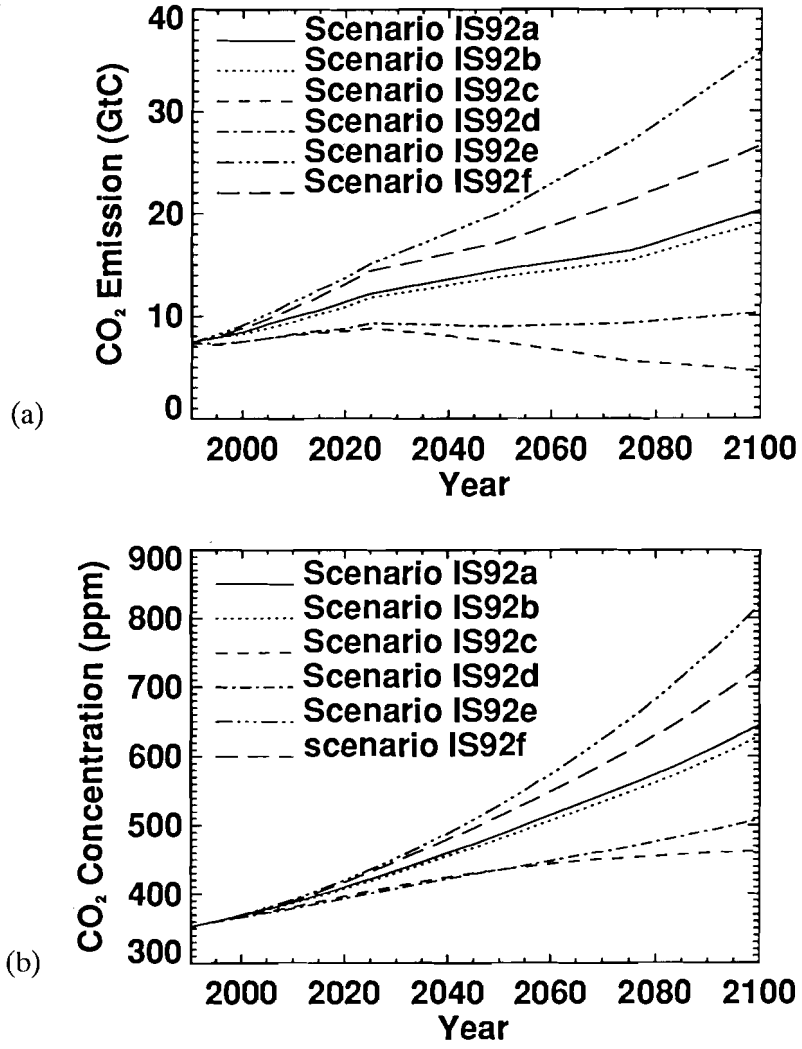

Fig. 5. Emission (a); and concentration (b) of CO_2 for IPCC (1992) scenarios, for 1990–2100.

for GWP are given in Table X for the constant emission scenario and the three representative IPCC scenarios. Since the disequilibrium enhancement is produced through the denominator CO_2 concentration in the expression for radiative forcing (IPCC, 1990; see Table 2.2),

$$\Delta F_{CO_2} = 6.3 \ln \left(\frac{c_{wp}(t)}{c_{wop}(t)} \right) , \tag{3}$$

no significant effect of gas identity upon GWP enhancement is expected. In Equation 3, c_{wp} and c_{wop} are the concentrations of CO_2 with and without pulse cases,

concentration among the scenarios become more apparent at longer times, the disequilibrium enhancement depends more strongly upon the emission scenario chosen with increasing time horizon. At a time horizon of 500 yr, the difference in disequilibrium enhancement thus ranges from 38% for IPCC Scenario IS92c to 165% for IPCC Scenario IS92e. Figure 5 shows that IPCC Scenario IS92e gives the largest CO_2 concentration and Scenario IS92c the smallest among all of the emission scenarios studied in the year 2100.

7. Combined GWP Effects of CO_2 Radiative Forcing Terms

We now estimate the range of combined uncertainties in GWP changes due to the balanced carbon cycle model, carbon cycle nonlinearities, and radiative forcing nonlinearities. Table XI shows the possible range of the combined uncertainties in GWP changes. The reference value of the combined uncertainties is obtained from the reference case of the balanced carbon cycle model ($\beta = 0.4$) with the IPCC (1992) CO_2-emission scenario, IS92a. The lower and upper limits of the combined uncertainties are estimated from the uncertainty limits of the biological feedback parameter $\beta = 0.2$ and 0.8 and the IPCC (1992) emission scenarios IS92c and IS92e which represent extrema for this study as shown in previous sections. The values in the table are the sum of the percentage differences between the model estimated equilibrium GWPs for IPCC scenarios and the IPCC (1992) equilibrium GWPs (first in bracket), the equilibrium GWPs for IPCC scenarios and the constant-emission scenario (second in bracket), and the disequilibrium and the equilibrium GWPs for IPCC scenarios (third in bracket). Both the systematic change in total uncertainty values and the range of possible effects on GWPs increase considerably as the time horizon for integration increases. The total increase in GWPs is 16% with about 4% range at a time horizon of 20 yr, but a time horizon of 500 yr gives a 110% increase with a possible range from 50 to 213%. This demonstrates that the dominant effect in the total systematic increase is the effect of using a disequilibrium atmosphere; in turn, the disequilibrium effect is strongly dependent upon the CO_2 emission scenario. The recent paper by Caldeira and Kasting (1993), however, shows that GWPs are nearly independent of the CO_2 emission scenario because of two major compensating effects of higher future atmospheric CO_2 concentration: one, the marginal radiative forcing per unit emission of CO_2 decreasing and two, the ocean's ability to absorb that CO_2 from the atmosphere diminishing. Caldeira and Kasting (1993), assumed only ocean sink for carbon in their calculations and the terrestrial biosphere was treated as neutral – neither a net source nor net sink. Our model results show that adding a biospheric sink to carbon cycle model will indeed affect GWPs – a pulse of CO_2 would decay much more rapidly in the short term than it would if only an ocean sink were assumed (Figure 4). This enhanced decay affects the integrated radiative forcing of CO_2 and hence GWPs.

concentration among the scenarios become more apparent at longer times, the disequilibrium enhancement depends more strongly upon the emission scenario chosen with increasing time horizon. At a time horizon of 500 yr, the difference in disequilibrium enhancement thus ranges from 38% for IPCC Scenario IS92c to 165% for IPCC Scenario IS92e. Figure 5 shows that IPCC Scenario IS92e gives the largest CO_2 concentration and Scenario IS92c the smallest among all of the emission scenarios studied in the year 2100.

7. Combined GWP Effects of CO_2 Radiative Forcing Terms

We now estimate the range of combined uncertainties in GWP changes due to the balanced carbon cycle model, carbon cycle nonlinearities, and radiative forcing nonlinearities. Table XI shows the possible range of the combined uncertainties in GWP changes. The reference value of the combined uncertainties is obtained from the reference case of the balanced carbon cycle model ($\beta = 0.4$) with the IPCC (1992) CO_2-emission scenario, IS92a. The lower and upper limits of the combined uncertainties are estimated from the uncertainty limits of the biological feedback parameter $\beta = 0.2$ and 0.8 and the IPCC (1992) emission scenarios IS92c and IS92e which represent extrema for this study as shown in previous sections. The values in the table are the sum of the percentage differences between the model estimated equilibrium GWPs for IPCC scenarios and the IPCC (1992) equilibrium GWPs (first in bracket), the equilibrium GWPs for IPCC scenarios and the constant-emission scenario (second in bracket), and the disequilibrium and the equilibrium GWPs for IPCC scenarios (third in bracket). Both the systematic change in total uncertainty values and the range of possible effects on GWPs increase considerably as the time horizon for integration increases. The total increase in GWPs is 16% with about 4% range at a time horizon of 20 yr, but a time horizon of 500 yr gives a 110% increase with a possible range from 50 to 213%. This demonstrates that the dominant effect in the total systematic increase is the effect of using a disequilibrium atmosphere; in turn, the disequilibrium effect is strongly dependent upon the CO_2 emission scenario. The recent paper by Caldeira and Kasting (1993), however, shows that GWPs are nearly independent of the CO_2 emission scenario because of two major compensating effects of higher future atmospheric CO_2 concentration: one, the marginal radiative forcing per unit emission of CO_2 decreasing and two, the ocean's ability to absorb that CO_2 from the atmosphere diminishing. Caldeira and Kasting (1993), assumed only ocean sink for carbon in their calculations and the terrestrial biosphere was treated as neutral – neither a net source nor net sink. Our model results show that adding a biospheric sink to carbon cycle model will indeed affect GWPs – a pulse of CO_2 would decay much more rapidly in the short term than it would if only an ocean sink were assumed (Figure 4). This enhanced decay affects the integrated radiative forcing of CO_2 and hence GWPs.

TABLE IX

Disequilibrium GWPs derived for several CO_2 emission scenarios using the best guess case (F(1980s) = 2.3 GtC/yr, $\beta = 0.4$) balanced carbon cycle model

(a) Constant-Emission Scenario GWPs at time horizon (years)					
Gas	20	50	100	200	500
CO_2	1.0	1.0	1.0	1.0	1.0
CH_4	39.7	24.1	15.3	10.0	6.2
N_2O	293.0	342.0	362.0	347.0	272.0
CFC-11	5120.0	5210.0	4600.0	3490.0	2240.0
CFC-12	8110.0	9320.0	9670.0	8980.0	6740.0
HCFC-22	4730.0	3280.0	2150.0	1410.0	879.0
CFC-113	5200.0	5940.0	6110.0	5590.0	4120.0
CFC-114	6900.0	8380.0	9480.0	10100.0	9490.0
CFC-115	6240.0	7890.0	9500.0	11400.0	13900.0
HCFC-123	384.0	200.0	126.0	82.0	51.2
HCFC-124	1790.0	986.0	621.0	405.0	253.0
HFC-125	5960.0	5630.0	4570.0	3240.0	2040.0
HFC-134a	3570.0	2460.0	1610.0	1050.0	658.0
HCFC-141b	2100.0	1300.0	829.0	541.0	338.0
HCFC-142b	4540.0	3580.0	2500.0	1650.0	1030.0
HFC-143a	5400.0	5680.0	5210.0	4120.0	2690.0
HFC-152a	606.0	315.0	198.0	129.0	80.8
CCl_4	2040.0	2010.0	1700.0	1240.0	786.0
CH_3CCl_3	406.0	219.0	138.0	90.1	56.3
CF_3Br	6400.0	6940.0	6650.0	5530.0	3720.0

(b) IPCC Scenario IS92e (High) GWPs at time horizon (years)					
Gas	20	50	100	200	500
CO_2	1.0	1.0	1.0	1.0	1.0
CH_4	39.8	24.8	16.9	12.6	9.7
N_2O	294.0	353.0	401.0	441.0	422.0
CFC-11	5130.0	5380.0	5080.0	4430.0	3480.0
CFC-12	8130.0	9620.0	10700.0	11400.0	10500.0
HCFC-22	4740.0	3390.0	2380.0	1790.0	1370.0
CFC-113	5210.0	6130.0	6750.0	7100.0	6410.0
CFC-114	6910.0	8660.0	10500.0	12800.0	14700.0
CFC-115	6260.0	8150.0	10500.0	14400.0	21600.0
HCFC-123	385.0	206.0	139.0	104.0	79.5
HCFC-124	1790.0	1020.0	686.0	514.0	393.0
HFC-125	5970.0	5820.0	5060.0	4110.0	3170.0
HFC-134a	3580.0	2540.0	1780.0	1340.0	1020.0
HCFC-141b	2100.0	1340.0	916.0	687.0	525.0
HCFC-142b	4550.0	3700.0	2760.0	2090.0	1600.0
HFC-143a	5420.0	5860.0	5760.0	5220.0	4180.0
HFC-152a	607.0	325.0	219.0	164.0	126.0
CCl_4	2050.0	2070.0	1880.0	1570.0	1220.0
CH_3CCl_3	407.0	226.0	153.0	114.0	87.4
CF_3Br	6420.0	7170.0	7350.0	7010.0	5790.0

TABLE IX

(continued)

(c) IPCC Scenario IS92a (Intermediate) GWP at time horizon (years)					
Gas	20	50	100	200	500
CO_2	1.0	1.0	1.0	1.0	1.0
CH_4	39.7	24.4	16.1	11.3	8.0
N_2O	293.0	347.0	382.0	395.0	348.0
CFC-11	5110.0	5300.0	4850.0	3970.0	2860.0
CFC-12	8100.0	9470.0	10200.0	10200.0	8610.0
HCFC-22	4730.0	3330.0	2270.0	1600.0	1120.0
CFC-113	5190.0	6030.0	6440.0	6360.0	5280.0
CFC-114	6890.0	8520.0	9990.0	11500.0	12100.0
CFC-115	6230.0	8020.0	10000.0	12900.0	17800.0
HCFC-123	383.0	203.0	132.0	93.2	65.5
HCFC-124	1780.0	1000.0	655.0	461.0	324.0
HFC-125	5950.0	5720.0	4820.0	3680.0	2610.0
HFC-134a	3560.0	2500.0	1700.0	1200.0	842.0
HCFC-141b	2090.0	1320.0	874.0	615.0	432.0
HCFC-142b	4540.0	3640.0	2630.0	1880.0	1320.0
HFC-143a	5390.0	5770.0	5490.0	4680.0	3440.0
HFC-152a	605.0	320.0	209.0	147.0	103.0
CCl_4	2040.0	2040.0	1790.0	1410.0	1000.0
CH_3CCl_3	405.0	223.0	146.0	102.0	71.9
CF_3Br	6390.0	7060.0	7010.0	6280.0	4760.0

(d) IPCC Scenario IS92c (Low) GWPs at time horizon (years)					
Gas	20	50	100	200	500
CO_2	1.0	1.0	1.0	1.0	1.0
CH_4	39.4	23.9	15.1	9.5	5.4
N_2O	291.0	340.0	360.0	330.0	237.0
CFC-11	5080.0	5180.0	4540.0	3320.0	1950.0
CFC-12	8050.0	9260.0	9550.0	8540.0	5870.0
HCFC-22	4700.0	3260.0	2120.0	1340.0	766.0
CFC-113	5160.0	5900.0	6020.0	5320.0	3590.0
CFC-114	6840.0	8330.0	9350.0	9620.0	8270.0
CFC-115	6190.0	7840.0	9370.0	10800.0	12100.0
HCFC-123	381.0	198.0	124.0	77.9	44.6
HCFC-124	1770.0	980.0	613.0	385.0	221.0
HFC-125	5910.0	5600.0	4510.0	3080.0	1780.0
HFC-134a	3540.0	2450.0	1590.0	1000.0	574.0
HCFC-141b	2080.0	1290.0	818.0	515.0	294.0
HCFC-142b	4510.0	3560.0	2470.0	1570.0	898.0
HFC-143a	5360.0	5640.0	5140.0	3920.0	2340.0
HFC-152a	601.0	313.0	196.0	123.0	70.4
CCl_4	2030.0	1990.0	1680.0	1180.0	685.0
CH_3CCl_{13}	403.0	218.0	136.0	85.7	49.0
CF_3Br	6350.0	6900.0	6560.0	5260.0	3240.0

TABLE X

Differences in disequilibrium GWPs (percent) from equilibrium GWPs for several model and emission scenarios

F_{oc}(1980s)/ GtC yr^{-1}	β	Emission case	Percent difference in GWPs at time horizon/yr 20	50	100	200	500
2.3	0.4	constant	5.4	10.8	18.6	32.2	62.8
2.3	0.4	IS92c	3.8	8.8	15.2	22.7	38.2
2.3	0.4	IS92a	4.5	11.5	24.7	52.1	114.5
2.3	0.4	IS92e	4.9	13.6	31.8	73.0	165.3

TABLE XI

Total uncertainty range of GWP changes in percent due to balanced carbon cycle model, carbon cycle nonlinearities, and use of disequilibrium atmospheres in CO_2 integrated radiative forcing calculations

Time horizon/yr	Lower limit	Reference value	Upper limit
20.0	13.3	15.7	19.9
	(8.8 − 0.3 + 4.5)	(10.5 + 0.7 + 4.5)	(11.6 + 2.7 + 5.6)
50.0	25.6	28.2	33.0
	(15.9 − 0.3 + 9.4)	(15.8 + 0.9 + 11.5)	(14.1 + 3.5 + 15.4)
100.0	34.8	40.5	44.3
	(19.5 − 0.3 + 15.0)	(15.4 + 0.4 + 24.7)	(5.2 + 1.0 + 38.1)
200.0	40.5	59.5	78.0
	(19.5 − 0.4 + 21.6)	(8.6 − 1.2 + 52.1)	(−14.5 − 5.3 + 97.8)
500.0	49.9	109.7	212.9
	(16.2 − 0.4 + 34.1)	(−1.9 − 2.9 + 114.5)	(−38.6 − 10.8 + 262.0)

8. Uncertainties in Atmospheric Lifetimes

The uncertainties in the atmospheric lifetimes of non-CO_2 greenhouse gases result from limitations in the measurements of emissions, loss processes, and atmospheric concentrations of the gases. There are no definitive evaluations of the range of lifetimes that would include all known measurement uncertainties. However, the combination of data from existing measurement programs with results from atmospheric models does provide a measure of the reasonable range of uncertainties in atmospheric lifetimes. The WMO (1991) international scientific assessment provides estimated uncertainty limits on most of the relevant greenhouse gases. The WMO recommended lifetime values and their error bounds are shown in Table I.